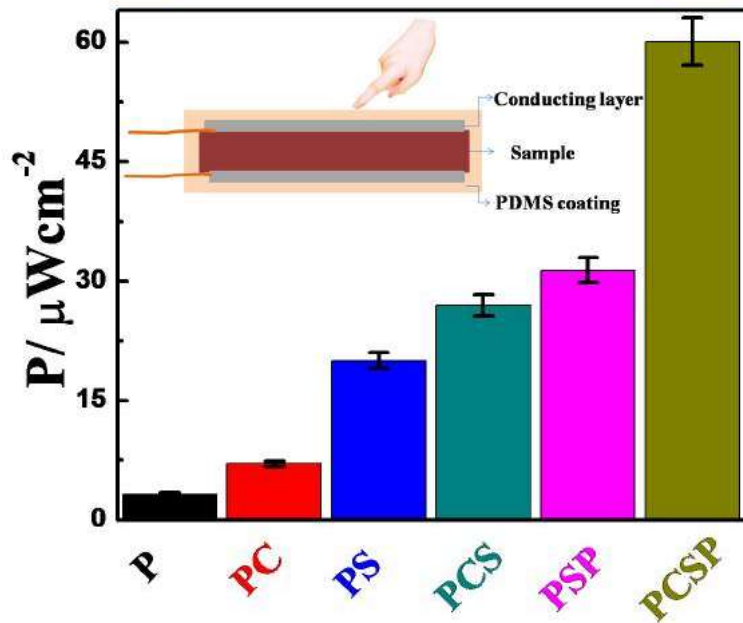
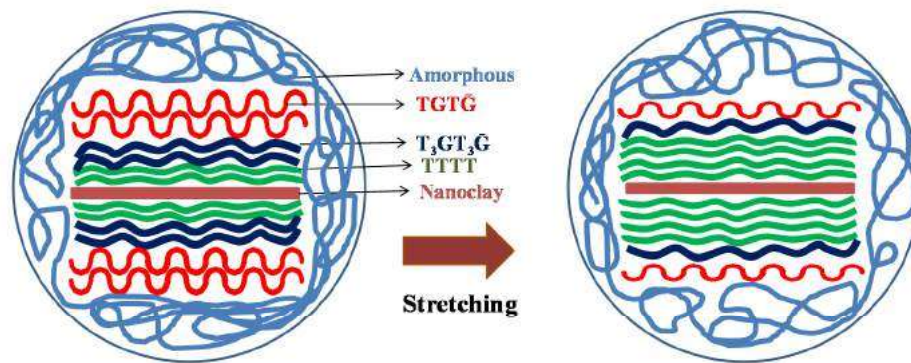


## Chapter 5

### Nanoparticle and Process Induced Piezoelectricity in Poly(vinylidene fluoride) Hybrid for Energy Harvesting



### 5.1. Introduction:

The electroactive  $\beta$ -phase in Poly(vinylfluoride) can be obtained by high pressure melt crystallization [162], high voltage poling [163], stretching [154], recrystallization [164] and molecular epitaxy on the surface of potassium bromide [165].  $\gamma$ -phase was prepared by Doll and Lando at high pressure crystallization, whose melting temperature is 15° higher than that of  $\alpha$  and  $\beta$ -phase [166]. The addition of two-dimensional layered nanoclay in PVDF matrix produces bulk piezoelectric materials which enhances the mechanical, physical and thermal properties as well [139, 167-169]. Two dimensional nanoclay has advantage for structural improvement than zero-dimensional fillers like titania and silica [135] where there is no change in structure or one dimensional filler like nanorod and CNT [136] where there is very less amount of  $\beta$ -phase due to dimensional constraints. PVDF crystallizes primarily in  $\alpha$ -phase in presence of two dimensional graphene sheets with very little amount of  $\beta$ -phase, which can also be proven from distinct spherulites in nanohybrid [170]. Hence, better compatibility and interaction between filler and polymer matrix is essential to generate electroactive phase in the polymer. Polar  $\beta$ -phase is the main reason behind the electronic properties whose measure is the piezoelectric coefficient.  $\beta$ -phase stabilization through melt intercalation in presence of organically modified nanoclay [167] shows increased stiffness from 1.3 to 1.8 GPa, along with the enhancement in elongation at break and toughness reported to be 140 and 700%, respectively, vis-a-vis pure PVDF [139]. The greater interaction is expected between polymer and nanoclay due to large surface area of nanoclay which promotes the formation of  $\beta$ -phase arising from better dispersion. Nanohybrids of nanoclay with amorphous polymer (PMMA) and polyurethane do not exhibit any change of structure

in presence of similar nature and content of nanoclay [90]. Similar study on structural change of PVDF in presence of cloisite 30B has been reported as  $\beta$  promoter agent [171].

Piezoelectric PVDF based devices are better to use when its piezoelectric properties can be enhanced by adding some nanofillers. Multi wall carbon nanotube (CNT) has been used as filler in PVDF and is found to be  $\beta$ -phase nucleating agent [172]. Use of carbon black in a hybrid of high density polyethylene-PVDF composite fibre has been shown for textile actuator [173]. Synthetic muscle fibre of cross section  $26 \text{ mm}^2$  produces  $0.5 \text{ N}$  actuation force from  $4.5 \text{ V}$ , sufficient to flex a human finger joint. A PVDF nanofiber, produced through electrospinning, generates an output voltage of  $6.3 \text{ V}$  under a pulse generated signal [174]. A flexible nanogenerator with single strand DNA and PVDF has been prepared and  $11 \text{ mW/cm}^2$  power density is reported through touch response [119]. In another study, a bilayer film has been prepared with poled PVDF-TrFE and graphene oxide, where the graphene oxide works as electrostatic component and its effect with piezoelectric component (poled PVDF-TrFE) is reflected in the output voltage as  $4 \text{ V}$  as compared to  $1.5 \text{ V}$  without graphene oxide layer [175]. So far, no such polymer robust film especially fluoropolymer / hybrid has been used as an energy harvesting material.

In this work, nanohybrids of poly(vinylidene fluoride) with 2D nanoclay has been prepared through solution route and the effect of elongation at moderately high temperature has been investigated for robust energy harvester. The extent of piezoelectric  $\beta$ -phase is enhanced by the incorporation of nanoclay and subsequent high temperature uniaxial controlled stretching. Phase change in processed hybrid has been shown through piezo force microscopy understanding the relative dimension. A unimorph for both pure PVDF and nanohybrid has been fabricated and their piezo- responses are evaluated. Finally, the power of the devices

under mechanical stress has been measured for its applicability in the real system. Morphology directed structural transformation with tougher and stiffer design nanohybrid developed here can be used to create multifunctional devices like sensors, actuators or other electromechanical self-powering devices.

## **5.2. Experimental:**

Materials: Poly(vinylidene fluoride) and organically modified clay, Cloisite 30B.

Nanohybrid of PVDF and nanoclay has been prepared by solution route as explained in **chapter 2**.

The pure PVDF and nanohybrids are termed as P and PC; stretched samples as P-S and PC-S; stretched and poled as P-SP and PC-SP.

## **5.3. Results and discussion**

### **5.3.1. Processing and nanoclay induced piezoelectricity**

Two synergistic approaches have been employed to induce piezoelectricity in PVDF as pure PVDF does not exhibit any piezoelectricity. All trans  $\beta$ -phase is known to be the reason behind piezoelectricity and, therefore, the particular  $\beta$ -phase has been generated in bulk PVDF by incorporating two dimensional nanoclay in the polymer matrix followed by controlled stretching of the film at high temperature to enhance the electroactive phase. The stress strain curve for pure PVDF and nanohybrid at high temperature (90 °C) is shown in **Figure 5.1a** indicating higher toughness and modulus of the nanohybrid as compared to pure PVDF. Toughness for nanohybrid increases to 101 MJ/m<sup>3</sup> from its value of 60 MJ/m<sup>3</sup> for

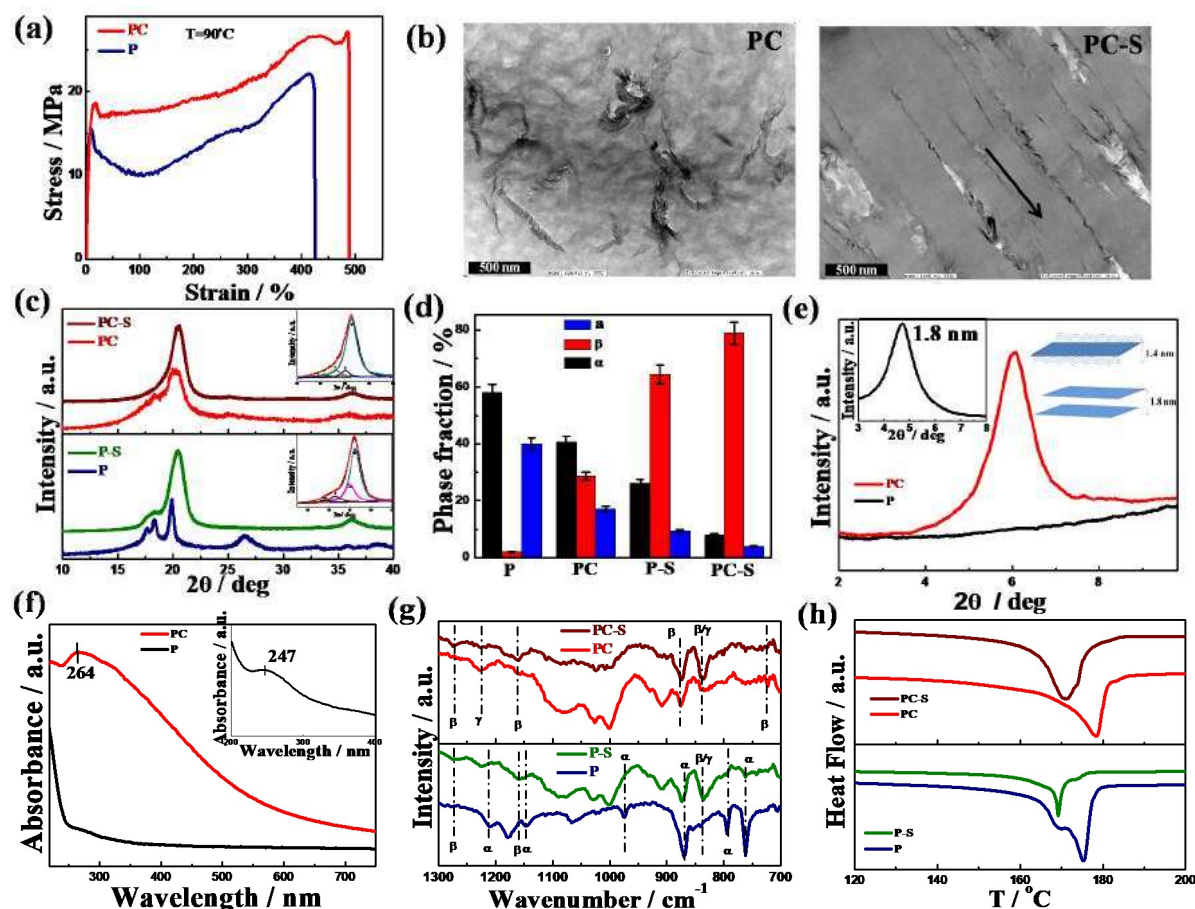


**Figure 5.1:** (a) Stress-strain curves and toughness for pure PVDF and nanohybrid at 90°C showing high elongation at break; (b) TEM images of nanohybrid before and after stretching (arrow indicates the stretching direction); (c) XRD patterns for pure PVDF and nanohybrid before and after stretching (inset shows deconvoluted diffractograms for stretched samples) and other deconvolution patterns have been shown in supporting information; (d) phase fraction from the deconvoluted patterns; a,  $\alpha$  and  $\beta$  represent the content of amorphous,  $\alpha$ - and  $\beta$ -phase, respectively; (e) XRD of PVDF and nanohybrid at lower angel, schematic shows the origin of diffraction peak (f) UV-visible spectra for pure PVDF and nanohybrid samples. Inset shows the UV-vis spectra for nanoclay (g) FTIR patterns of PVDF and nanohybrid before and after stretching indicating the presence of different phases; and (h) DSC thermograms of PVDF and nanohybrid before and after stretching showing the change in melting temperature due to phase change.

pure PVDF at the same temperature of measurement. It is important to mention that toughness values have considerably increased at high temperature with significantly higher elongation at break as compared to room temperature measurement raising a situation of

extensive uncoiling (stretching out) of PVDF chain which leads to the formation of all trans  $\beta$ -phase. At room temperature, the toughness of pure PVDF and nanohybrid is 2 and 6 MJ/m<sup>3</sup> respectively. Higher elongation at break (420 and 490% for P and PC, respectively) at high temperature is presumably due to low viscosity while greater elongation for nanohybrid lies in its needle like morphology in presence of nanoclay as discussed later [154]. Stretching has a significant role to align the nanoparticle, in addition to polymer chain, in the direction of force field as evident from the orientation of nanoclay in TEM images in the stretching direction as opposed to the random orientation of as prepared nanohybrid (**Figure 5.1b**). However, the nanoclay platelets are well dispersed in PVDF matrix with greater tactoid dimension in as prepared nanohybrid while oriented and smaller dimension tactoid is noticed after stretching lead to the formation of better epitaxial crystallization of PVDF chain on top of a large number of smaller tactoids in nanohybrid after stretching.

Nanoclay in hybrid nucleates piezoelectric  $\beta$ -phase ( $2\theta \sim 20.5^\circ$ ; 200/110 planes) in PVDF against absolute  $\alpha$ -phase ( $17.6^\circ$  (100),  $18.3^\circ$  (020) and  $19.9^\circ$  (110) planes) crystalline state in pure PVDF before stretching (**Figure 5.1c**) [139]. Interestingly, phase conversion occurs during stretching and considerable  $\beta$ -phase appears both in pure PVDF and its nanohybrid. XRD peak in nanohybrid at  $36.4^\circ$  also indicates the formation of  $\beta$ -phase, whose intensity enhances after stretching, with the disappearance of peaks of pure PVDF at  $33.0^\circ$  and  $37.22^\circ$ . Representative deconvolution of stretched samples has been shown in the inset figure from where the extent of various phases have been calculated and plotted in **Figure 5.1d** showing greater extent of  $\beta$ -phase after stretching and nanohybrid exhibit as high as 80% of  $\beta$ -phase, suitable for any piezoelectric devices. The appearance of a new peak at  $2\theta \sim 19.2^\circ$  in presence of nanoclay is due to the formation of a distorted  $\beta$ - or  $\gamma$ -conformation, another electroactive

phase of PVDF [140]. However, it is evident from XRD patterns that nanoclay induces piezoelectric phase in nanohybrid while elongation significantly enhances the electroactive phase content and predominantly the  $\beta$ -phase crystallizes on top and bottom of silicate layers arising from good interactions between nanoclay and polymer chain leading to a strong band at  $2\theta \sim 6.03^\circ$ , appears from sandwiching the nanoclay layers with PVDF crystals (**Figure 5.1e**) [90]. The interaction of polymer and nanoclay is revealed from UV-visible spectroscopy from the shifting of the absorption peak at 247 nm of pristine nanoclay to 264 nm in nanohybrid **Figure 5.1f**. This is to mention that absorption peak of pristine nanoclay appears from the olefinic double bond present in the organic modifier of the nanoclay while pure PVDF does not show any absorption band in the energy range studied. Higher elongation at break or greater draw ratio [90] augment the molecular alignment in the direction of force field and greater alignment helps the PVDF chains to crystallize in microfibrillar all-trans planar zigzag conformation of  $\beta$ -phase. The conversion of amorphous and  $\alpha$ -phase into  $\beta$ -phase due to stretching is evident from the fact that considerable reduction of amorphous and  $\alpha$ -phase content after elongation both in PVDF and nanohybrid facilitated at high temperature ( $90^\circ\text{C}$ ) due to greater mobility [56, 144]. The structural change over is also verified through FTIR peaks at 837, 875 and  $1274\text{ cm}^{-1}$ , assigned to  $\beta$ -peaks, after stretching against predominant  $\alpha$ -peaks at 762, 795, 868, 973, 1148 and  $1210\text{ cm}^{-1}$  before stretching in pure PVDF (**Figure 5.1g**) [140, 158]. On the other hand, nanohybrid shows all the above  $\beta$ -peaks including new  $\beta$ -peaks at 725,  $1163\text{ cm}^{-1}$  and  $\gamma$ -peak at  $1224\text{ cm}^{-1}$  with the disappearance of corresponding  $\alpha$ -peaks as commensurate from XRD studies. However,  $\alpha$ - and amorphous phases are converted into  $\beta$ -phase after stretching in pure PVDF while the piezoelectric phase already exists in nanohybrid and its extent increases significantly after

uniaxial stretching. Melting endotherm of stretched PVDF exhibits peak at 169.0 °C against melting point of unstretched PVDF at 175.2 °C, corresponding to the  $\beta$ - and  $\alpha$ -phase of PVDF after and before stretching, respectively (**Figure 5.1h**). This is to mention that double melting endotherms of pure PVDF before stretching is due to melt recrystallization. On the other hand, nanohybrid before stretching shows peak at 178.3 °C, which may be attributed to the formation of  $\gamma$ -phase along with  $\beta$ -phase while the peak position has shifted to 170.7 °C after stretching suggesting the transformation into  $\beta$ -phase although considerable  $\gamma$ -phase exist in nanohybrid as observed through XRD and FTIR measurements [53, 176]. The increment in heat of fusion after stretching (39.1 to 44.9 Jg<sup>-1</sup> for PVDF and 37.5 to 43.0 Jg<sup>-1</sup> in nanohybrid) suggests conversion from amorphous to crystalline ( $\beta$ -phase) during stretching. However, there is more conversion from amorphous to  $\beta$  in nanohybrid after stretching while in PVDF it is predominantly  $\alpha$  to  $\beta$ .

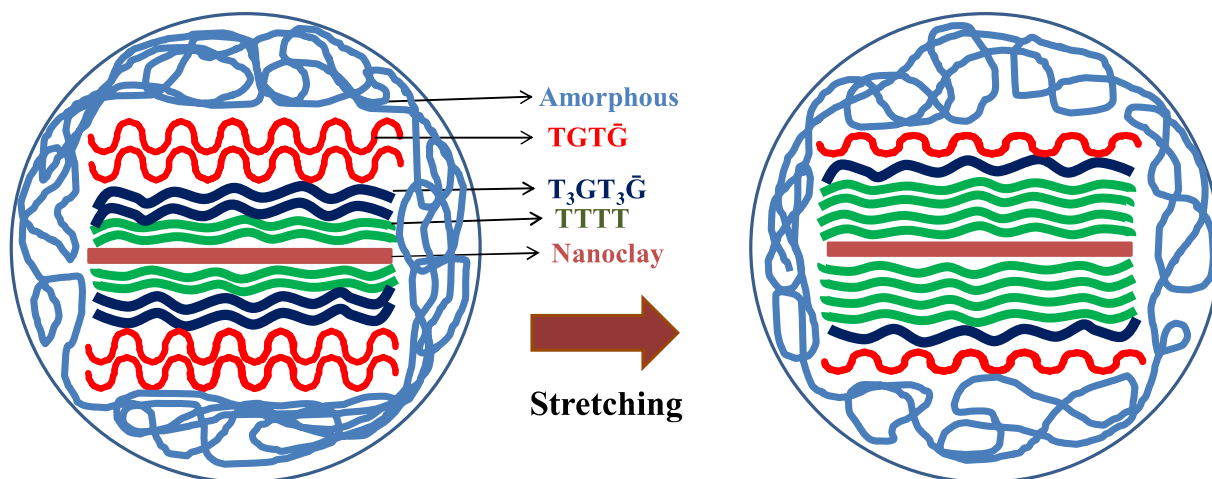


**Figure 5.2:** Schematic representation of phase transformation in nanohybrid and change in structure of single island or domain.

Structural, spectroscopic and thermal measurements strongly indicate the induced piezoelectric phase in PVDF whose extent significantly increase in the presence of nanoclay

after stretching providing good amount of electroactive phase in the material suitable for its use as piezo-device and a schematic representation of phase change during stretching is shown in **Figure 5.2** indicating large extent of polymer crystallize on top of nanoclay surface in  $\beta$  and  $\gamma$ -phase against meagre amount of  $\beta$ -phase in pure PVDF after stretching. Hence,  $\beta$ -phase lies like islands in the polymer matrix and act as electroactive phase having large variation in size and shape in pure PVDF and its nanohybrid especially after stretching.

### 5.3.2. Morphology and mapping of piezo-phase

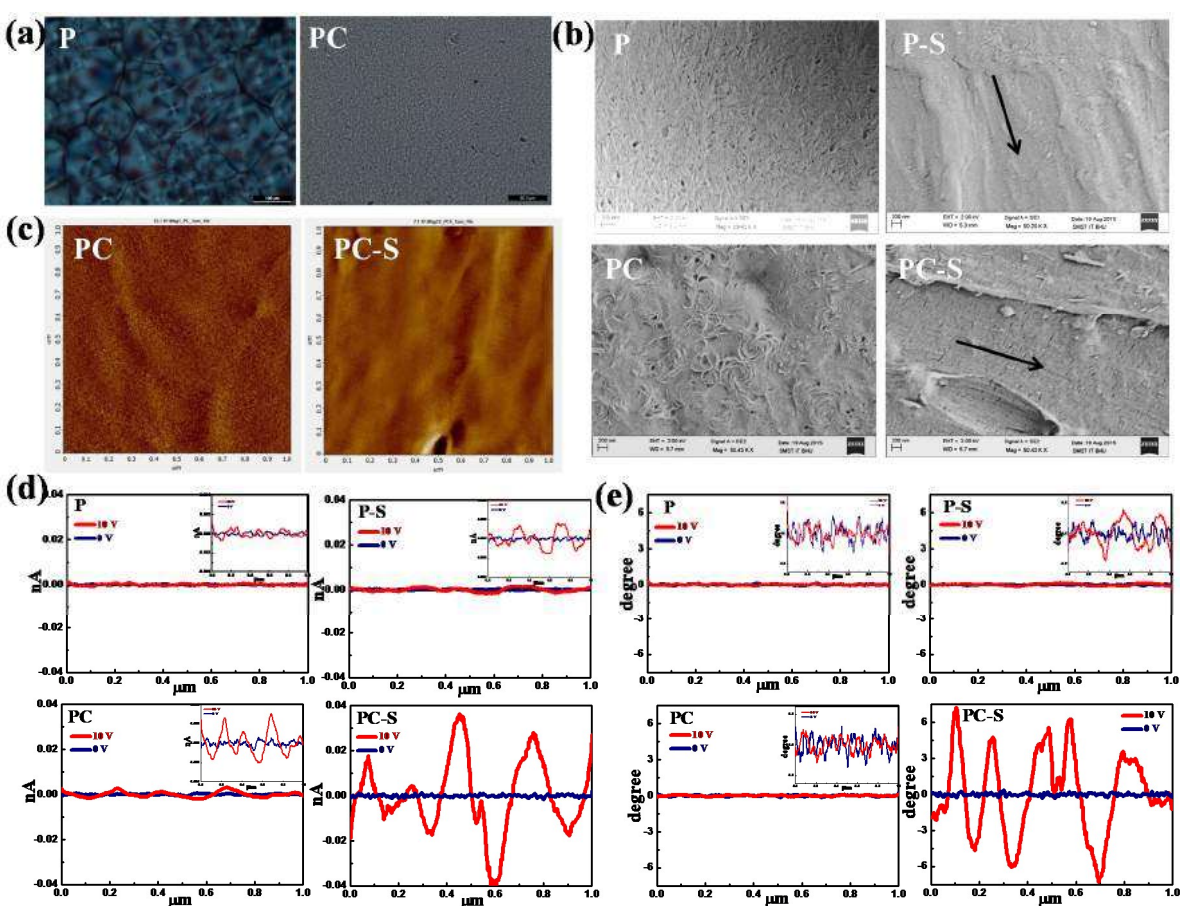
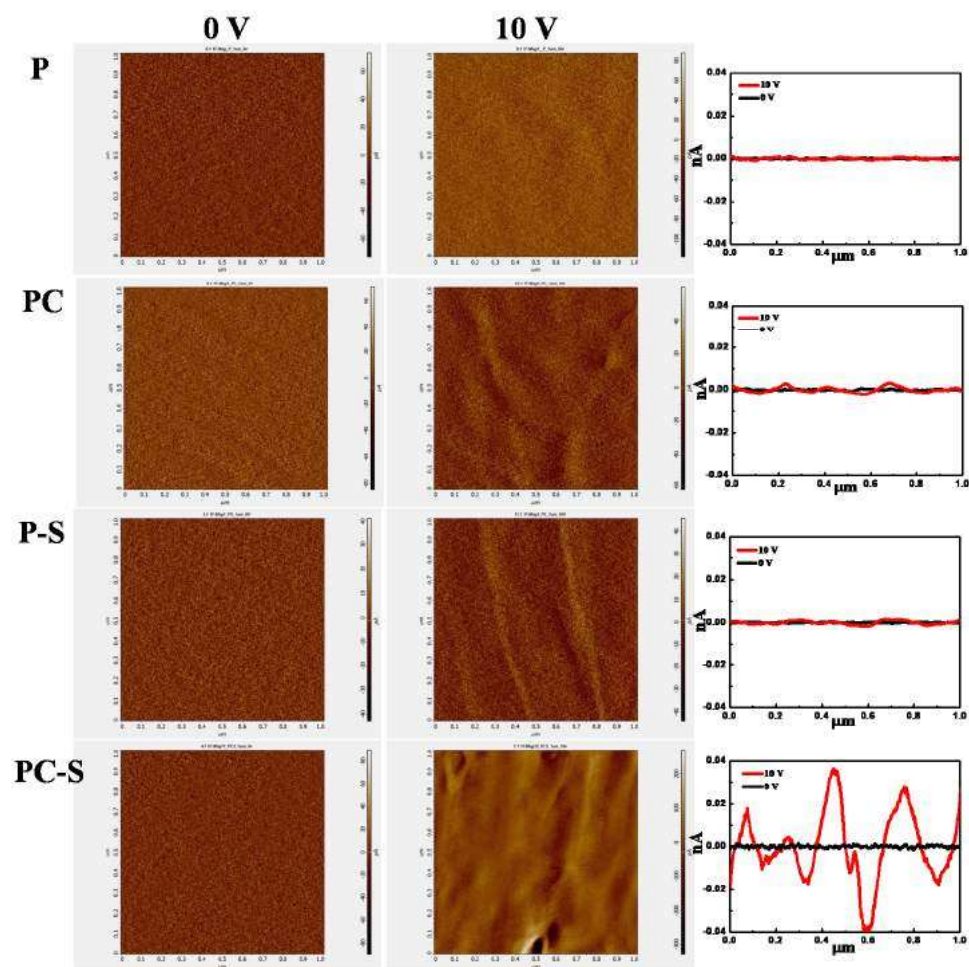


**Figure 5.3:** (a) Polarized optical microscope images of pure PVDF and its nanohybrid showing spherulite in pure PVDF and no birefringence in nanohybrid; (b) SEM images of pure PVDF and nanohybrid before and after stretching indicating the direction of stretching; (c) Piezo force microscopy images of nanohybrid samples before and after stretching; (d) Piezo force microscopy of P, PC, P-S and PC-S samples showing average profiles of magnitude; and (e) phase angle of the indicated samples. Inset figure suggests the magnified view of the respective profiles.

The crystalline phases are revealed from polarized optical micrographs. Well defined spherulites of  $\alpha$ -phase can be seen in pure PVDF against birefringence less morphology due to tiny needle like crystallites of  $\beta$ -phase in nanohybrid (**Figure 5.3a**) [146]. Morphology at high magnification is observed through scanning electron microscope, which also supports the spherulitic pattern in unstretched PVDF and the mesh like morphology in nanohybrid (**Figure 5.3b**). The oriented pattern is evident in the stretched samples (shown by the arrows) suggesting the molecular reorganization due to stretching towards force field and this orientation of molecules help crystallizing in  $\beta$ -phase during stretching. The surface morphology is also studied through piezo force microscopy (PFM) at a bias voltage of 10 V and compared the morphology in absence of any potential (**Figure 5.3c**). Shredded morphology is noticed in case of PC (before stretching) presumably due to  $\beta$ -phase whose extent enhances considerably after stretching (PC-S) as opposed to the non-shredded surface morphology of pure PVDF (**Figure 5.4**). Average profiles for magnitude and phases are shown in **Figure 5.3d & e**. We can see from **Figure 5.4** that there is almost no change in magnitude as well as phase in pure PVDF before and after applying the bias voltage in absence of any piezo phase while there are considerable changes of magnitude and phase in P-S (stretched PVDF) and PC after applying the bias voltage, as evident from the enlarge section as shown in the inset, arising from the modest amount of  $\beta$ -phase (64%) there.

Interestingly, significant changes of magnitude and phase are noticed in PC-S (stretched nanohybrid),  $\sim 0.04$  nA and  $\sim 7.5$  degree, after the application of bias voltage confirm the presence of large extent of  $\beta$ -phase (80%) as compared to unstretched sample and pure PVDF. Further, the average size of piezo-domain, as calculated from the width of individual peak profile, is around 110 nm while the greater intensity of profile peak indicates the

consolidation of the  $\beta$ -phase and found to be maximum in PC-S. PFM images of various samples and corresponding phase and magnitude are shown in **Figure 5.4** showing clear piezoelectric domains.



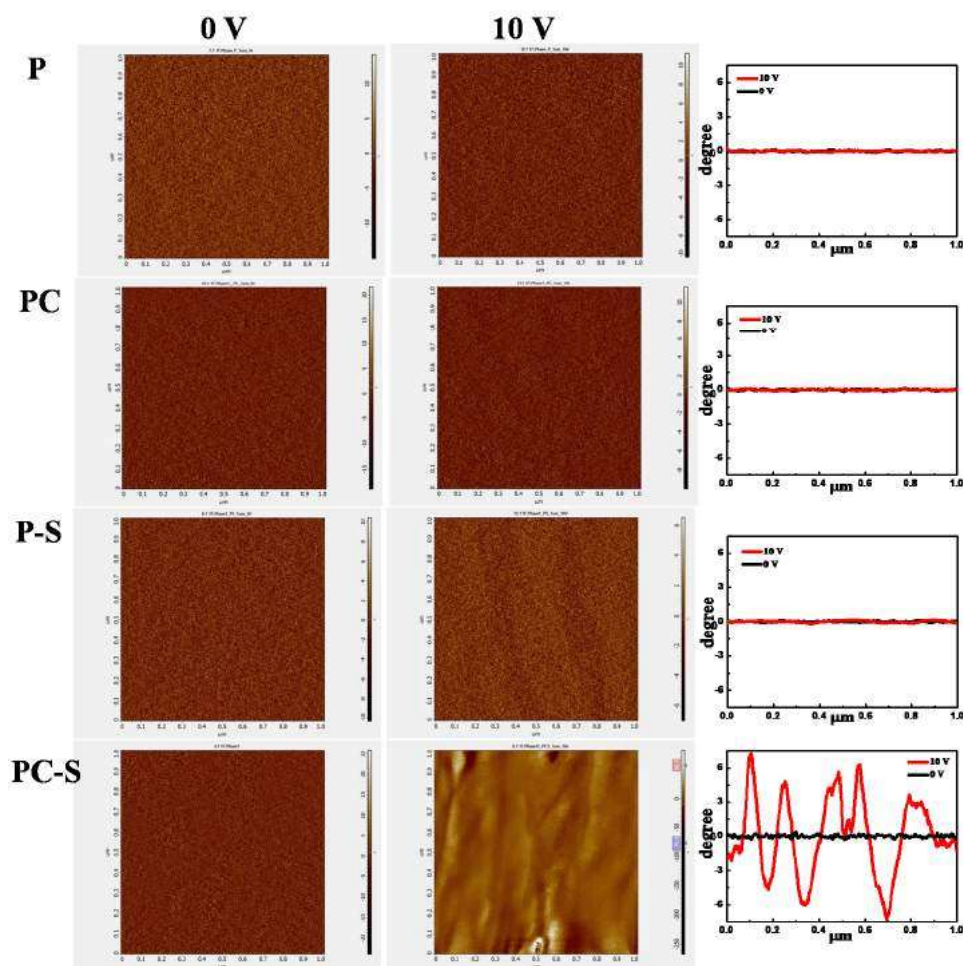


**Figure 5.4:** Average profiles for (a) magnitude and (b) phase of P, PC, P-S and PC-S.

However, it is evident that nanoclay and stretching generate piezoelectric phase and the material is expected to show the piezoelectricity. Schematics of phase transformations in nanohybrid are shown in **Figure 5.2**. Polymer molecules crystallize on top and bottom of the layered silicates in nanohybrid. Further,  $\beta$ -phase crystallizes just on top of nanoclay or clay stacks presumably due to greater interaction followed by distorted  $\beta$ - or  $\gamma$ -phase, as the interaction gradually diminish and ultimately conventional  $\alpha$ -phase appear in the top layer. These different phases make an island type of structure surrounded by the amorphous phase of polymer. All the phases try to convert into  $\beta$ -phase after stretching and the amount of  $\alpha$ -

and amorphous phase decreases considerably (**Figure 5.2**). The extent of piezoelectric phase is quite less before stretching which increases significantly after stretching due to formation of electroactive  $\beta$ -phase.

### 5.3.3. Piezoelectric responses

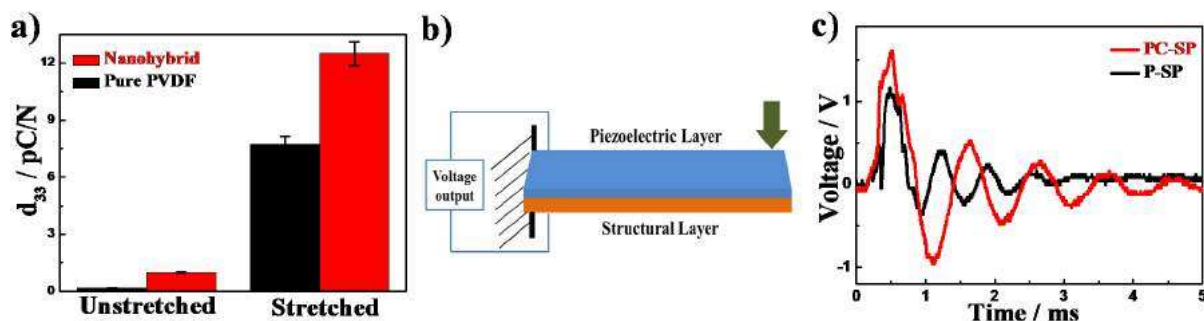


**Figure 5.5:** (a) enhancement in piezoelectric coefficient of samples after stretching; (b) schematic of unimorph made by stretched and poled film samples; and (c) comparison of output voltage measured by impact load.

It is clear from the structural and morphological measurements that developed nanohybrid is piezoelectric in nature and the piezoelectric phase has been increased through uniaxial stretching. The piezoelectric coefficient,  $d_{33}$  is an imperative parameter to measure the piezoelectricity of any material. **Figure 5.5a** shows  $d_{33}$  values for both unstretched and stretched samples after poling at an electric field of 600 kV/cm. The unstretched samples show very low  $d_{33}$  values of 0.2 and 1 pC/N for pure PVDF and nanohybrid, respectively. The respective values increase considerably to 7.7 and 12.5 pC/N after stretching indicating the significant improvement in piezoelectricity due to induction of  $\beta$ -phase in presence of nanoclay and further enhancement due to uniaxial stretching. However, it is clear that higher  $\beta$  content samples exhibit higher  $d_{33}$  values, which is suitable for the piezoelectric devices. As the piezoelectric effect originates from induced polarization and to induce more

polarization after stretching, the dipoles are oriented by electric poling with a strong electric field at an elevated temperature. The piezoelectric properties are directly related to the degree of polarization achieved. High temperature helps minimizing the warping due to relaxation of polymer and helps it to alter in a new volume. There is an optimum poling temperature which gives maximum polarization, unlike the poling field where larger value will give larger polarization [177, 178]. However, we have chosen the optimum condition for better piezoelectricity.

A device has been fabricated as explained in the experimental section having the unimorph of high piezoelectric coefficient. **Figure 5.5b** shows the representative assembly of the device combining the structural and electroactive layers and impulse load is applied in one end through cantilever. The voltage responses under impulse load are compared for stretched and poled PVDF and its nanohybrid samples (**Figure 5.5c**). Nanohybrid (PC-SP) exhibits higher output voltage (1.6 volts) as compared to 1.1 volts using PVDF (P-SP). Further, the piezo response dies out in just 3 ms in P-S sample while PC-S shows the response time up to 6 ms indicating superior device activity using nanohybrid arising from its greater extent of piezoelectricity.

#### **5.3.4. Energy harvesting**

The developed hybrid piezoelectric material has been utilized for energy harvesting by measuring the power output under the external load on to the material and compare the efficiencies. Piezoelectric films (both unstretched, stretched and poled) of dimension 1x1 cm<sup>2</sup> are coated with silver for making attachment to the electrodes and the device has been

prepared as discussed in **Chapter 2**, experimental section. The stress on the device has been applied by finger pressing. The open circuit voltage of samples were measured and the data

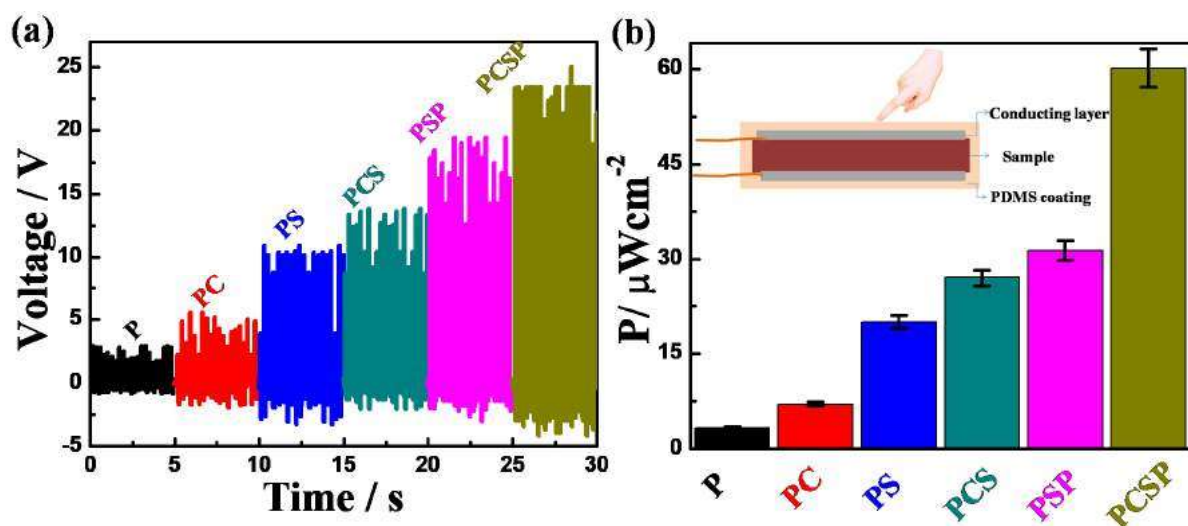


**Figure 5.6:** (a) open circuit voltage for unstretched, stretched and poled samples of pure PVDF and nanohybrid and (b) corresponding power density of the samples.

is shown in **Figure 5.6a**. The highest peak to peak open circuit voltage is obtained for stretched and poled nanohybrid sample of ~30 V as compared to ~4 V for pure PVDF. Also, the corresponding power density is 60μW/cm<sup>2</sup>. The high voltage and power output corresponds to the higher piezoelectric phase and also because of the effect of poling as discussed in **chapter 4**.

On application of external force, the crystal structure of the polymer film is deformed, resulting in induction of piezoresponse by interchanging the deformed structure to a stable one or vice versa. β-phase PVDF molecules are self-polarized (all trans configuration) along a direction even in absence of any external electric field, the combined effect of stress and surface charge induce polarization results in a self-powered flexible piezoelectric energy harvester. Nanohybrid layers experience appropriate strain upon impact with the load

produce deformation in its crystal structure that leads to piezopotential across the surface and contribute to an electric output signal. This creates a piezo-potential on each side of nanohybrid layer inducing a charge cloud and this potential difference leads to a flow of electron in external circuit, appears in observed output voltage.

In **Figure 5.6b**, we can see that the power density systematically increases; the relative increment is due to greater electroactive  $\beta$ -phase in presence of nanoclay and subsequent stretching and in poled samples due to the alignment of dipoles. However, PVDF nanohybrid with much improved electroactive  $\beta$ -phase has every potential for its use as energy harvester with easy processing and cost effectiveness. However, our devices using stretched nanohybrid generates maximum power of  $60 \mu\text{W}/\text{cm}^2$ , which is more than sufficient to use it as biomechanical energy harvester from human body and has vast application in health monitoring systems to be used as sensors.

#### **5.4. Conclusion**

The nanohybrid of PVDF with organically modified nanoclay has been prepared through solution route and good dispersion of nanoclay in polymer matrix is confirmed through transmission electron microscopy. Uniaxial elongation at high temperature shows greater breaking strain in nanohybrid where oriented pattern of nanoclay is noticed, responsible for its greater toughness, measured from area under the stress-strain curve. Nanoclay induces piezoelectric  $\beta$ -phase and polymer chain crystallizes on the surface of nanoclay and further conversion is done through uniaxial stretching at high temperature. The piezoelectric  $\beta$ -phase in nanohybrid has increased up to 80% in nanohybrid as measured from the deconvoluted XRD patterns. The structural changes, either by nanohybrid formation or stretching, are

confirmed through XRD, FTIR, POM, SEM and DSC studies. Mapping of piezoelectric domain is performed through piezo force microscopy, under a bias potential, with the dimension of 110 nm in stretched nanohybrid as opposed to zero size dimension in pure PVDF. The higher piezoelectric coefficient also reflects from higher piezoelectric  $\beta$ -phase in nanohybrid. Unimorphs were made with high piezoelectric coefficient material exhibiting better piezoelectric device performance from stretched nanohybrid. Devices are fabricated and open circuit voltage and power density is measured. The stretched and poled nanohybrid shows the highest open circuit voltage of  $\sim 30$  V and power density of  $60 \mu\text{W}/\text{cm}^2$  on finger tapping. This amount of power is sufficient to power the micro-electronic devices. In brief, novel piezoelectric polymer nanohybrid is developed using PVDF and nanoclay with easy processing which have high energy output and has great values for future applications.